DALTON
FULL PAPER

Low temperature kinetic study of very fast substitution reactions at platinum(II) *trans* to olefins †

Stefanus Otto ‡ and Lars I. Elding *

Inorganic Chemistry, Chemical Center, Lund University, P. O. Box 124, SE-221 00 Lund, Sweden. E-mail: LarsI.Elding@inorg.lu.se

Received 4th January 2002, Accepted 19th March 2002
First published as an Advance Article on the web 2nd May 2002

Ultra-fast substitution of chloride for bromide, iodide, azide and thiocyanate *trans* to ethene in Zeise's anion, $[PtCl_3(C_2H_4)]^-$, **1**, has been investigated in methanol solvent by use of cryo temperature diode array stopped-flow spectrophotometry. Reactions follow the usual two-term rate law for square-planar substitutions, $k_{obs} = k_1 + k_2[Y]$ (where $k_1 = k_{MeOH}[MeOH]$), with $k_1 = 118 \pm 10$ s^{-1} and $k_2 = (5.1 \pm 0.2) \times 10^2$, $(3.51 \pm 0.07) \times 10^3$, $(11.8 \pm 0.2) \times 10^3$, and $(56 \pm 4) \times 10^3$ mol^{-1} dm^3 s^{-1} for Y = Br$^-$, I$^-$, N_3^- and SCN$^-$, respectively, at 223 K. Activation parameters for MeOH, Br$^-$, I$^-$ and N_3^- are $\Delta H^{\neq} = 23 \pm 2$, 21 ± 2, 17 ± 1.0 and 11.9 ± 1.5 kJ mol^{-1} and $\Delta S^{\neq} = -124 \pm 10$, -96 ± 9, -98 ± 4 and -111 ± 6 J K^{-1} mol^{-1}, respectively. Recalculation of k_1 to second-order units gives the sequence of nucleophilicity MeOH < Br$^-$ < I$^-$ < N_3^- < SCN$^-$ (1 : 100 : 700 : 2500 : 12000) at 223 K. This nucleophilic discrimination decreases with increasing temperature. Chloride for iodide substitution *trans* to allyl alcohol, vinyltrimethylsilane and cyclooctene at $[PtCl_3(L)]^-$, (L = CH_2CHCH_2OH, **2**; $CH_2CHSiMe_3$, **3**; C_8H_{14}, **4**) follow the same rate law with $k_1 = 116 \pm 5$, 31.0 ± 0.3 and 23.6 ± 0.1 s^{-1} and $k_2 = (2.65 \pm 0.06) \times 10^3$, $(0.273 \pm 0.005) \times 10^3$ and $(0.119 \pm 0.002) \times 10^3$ mol^{-1} dm^3 s^{-1} at 223 K. Activation parameters are $\Delta H^{\neq}(k_{MeOH}) = 24.4 \pm 1.3$, 28.4 ± 0.6 and 29.9 ± 0.8 kJ mol^{-1}, $\Delta S^{\neq}(k_{MeOH}) = -120 \pm 5$, -114 ± 2 and, -108 ± 3 J K^{-1} mol^{-1}, $\Delta H^{\neq}(k_2) = 19.9 \pm 1.2$, 24.6 ± 1.7 and 24 ± 3 kJ mol^{-1} and $\Delta S^{\neq}(k_2) = -88 \pm 5$, -84 ± 7 and -93 ± 10 J K^{-1} mol^{-1}, for **2**, **3** and **4** respectively. The free energies of activation are dominated by the $-T\Delta S^{\neq}$ terms. The crystal and molecular structures of $Bu_4N[PtCl_3(CH_2CHSiMe_3)]$ and $Bu_4N[PtCl_3(C_8H_{14})]$ show slight Pt–Cl bond lengthening to 2.314(2) Å and 2.3238(16) Å *trans* to the olefins, similar to that found *trans* to ethene in Zeise's anion. All experiments support a model for the very fast substitution reactions *trans* to the olefins in which ground state labilisation is much less significant than transition state stabilisation. Extrapolation to ambient temperature together with literature data for related reactions in methanol solvent gives a quantitative measure of the *trans* effect of ethene as: $SR_2 < Me_2SO < AsEt_3 < PR_3 < P(OR)_3 < C_2H_4$ (1 : 5 : 400 : 3500 : 7000 : 3×10^6). The relative *trans* effect of the olefins studied is $C_2H_4 \sim CH_2CHCH_2OH > CH_2CHSiMe_3 \sim C_8H_{14}$, spanning a factor of between 5 and 30 depending on the nucleophile, and reflecting minor differences in steric and electronic properties of the olefins.

Introduction

It is well known that ligand substitution processes *trans* to olefins are extremely rapid due to the high π *trans* effect of these ligands.[1] Quantitative studies of direct substitution kinetics *trans* to olefins in unhindered systems such as Zeise's anion, $[PtCl_3(C_2H_4)]^-$, **1**, do not seem to have been published so far. Preliminary temperature jump experiments in our laboratory 25 years ago indicated an approximate half-life for the hydrolysis of the *trans* chloride of **1** as short as 5×10^{-5} s in aqueous solution at 25 °C.[2] Based on that rough estimation and related kinetics data, a *trans* effect order $H_2O : Cl^- : Me_2SO : C_2H_4$ of $1 : 330 : 2 \times 10^6 : \sim 10^{11}$ was derived.[2] Tobe and co-workers, using sterically hindered substituents resulting in much slower reactions, estimated a qualitative *trans* effect sequence as $R_2S < R_2SO < PR_3 < P(OR)_3 < CO < C_2H_4$.[3]

We have previously studied the ethene exchange at Zeise's anion, $[PtCl_3(C_2H_4)]^-$, **1**,[4] and have postulated a mechanism in which the very labile chloride ligand co-ordinated *trans* to the ethene is involved in the exchange process. It was therefore of interest to investigate the very fast substitution kinetics of chloride *trans* to ethene directly. We report here studies of such reactions of complex **1** as well as of the related olefinic complexes $[PtCl_3(L)]^-$, L = CH_2CHCH_2OH (allyl alcohol), **2**; $CH_2CHSiMe_3$ (vinyltrimethylsilane), **3** and C_8H_{14} (cyclooctene), **4**. These studies were made feasible by use of recently developed reliable low temperature stopped-flow diode-array equipment. The experiments give, for the first time, a quantitative evaluation of the kinetic parameters for the very fast substitution processes *trans* to olefins co-ordinated to platinum(II) in sterically unhindered systems. A quantitative measure of the *trans* effect of ethene and related olefins compared to other *trans*-labilising ligands can also be derived from the kinetics data. In order to elucidate the relative importance of ground state and transition state effects for the reactivity, the crystal and molecular structures of the tetrabutylammonium salts of **3** and **4** have also been determined.

Experimental

Chemicals

Allyl alcohol (ACROS, 99+%), vinyltrimethylsilane (Fluka, >97%) and cyclooctene (ACROS, 95%) were dried over molecular sieves, while ethene (AGA, 99.95%) was used as received. Methanol solvent of analytical grade (Riedel-de Haën) was

† Electronic supplementary information (ESI) available: observed pseudo-first order rate constants for all reactions investigated, absorbance *versus* chloride concentrations for the K_{Cl} determinations. See http://www.rsc.org/suppdata/dt/b2/b200197g/

‡ On leave from University of the Free State, P.O. Box 339, Bloemfontein 9300, South Africa.

 DOI: 10.1039/b200197g

freshly distilled from CaH_2 under dinitrogen prior to use. Analytically pure NaBr (Mallinckrodt), NaI (Merck), NaN_3 (BDH) and NaSCN (Mallinckrodt) were used as received. Anhydrous $NaClO_4$ (ACROS) was used to maintain a constant ionic strength. Silver triflate (Aldrich) was used for halide abstraction reactions and analytical grade LiCl (Merck) was used as a source of chloride in the determination of equilibrium constants K_{Cl}.

Preparation of complexes

$K[PtCl_3(C_2H_4)]$ was prepared according to literature procedures.[5] The tetrabutylammonium salt of **1** was prepared as reported previously,[4] while complexes **2**–**4** were prepared by substitution of C_2H_4 from $Bu_4N[PtCl_3(C_2H_4)]$ by addition of a slight excess of the appropriate olefin in acetone medium.[6] Complexes **2** and **3** were purified by recrystallisation from a mixture of dichloromethane/diethyl ether (1 : 2) while **4** was obtained as a crystalline solid directly by evaporation of the acetone reaction medium.

$Bu_4N[PtCl_3(C_2H_4)]$. ^{1}H NMR: 1.04 (t, 12H), 1.48 (m, 8H), 1.67 (m, 8H), 3.28 (m, 8H), 4.41 (t, 4H, $^{1.5}J_{Pt-H}$ = 64 Hz). ^{195}Pt NMR: −2755. ^{13}C NMR: 13.73 (4C, CH_3), 19.74 (4C, CH_2), 24.11 (4C, CH_2), 58.94 (4C, CH_2), 68.22 (2C, =CH_2, $^1J_{Pt-C}$ = 193 Hz).

$Bu_4N[PtCl_3(CH_2CHCH_2OH)]$. ^{1}H NMR: 1.04 (t, 12H), 1.49 (m, 8H), 1.66 (m, 8H), 3.25 (m, 8H), 4.13 (tm, 2H, $^{1.5}J_{Pt-H}$ = 53 Hz), 4.40 (m, 1H), 4.55 (m, 1H), 5.42 (m, 1H, $^{1.5}J_{Pt-H}$ = 66 Hz). ^{195}Pt NMR: −2681. ^{13}C NMR: 13.67 (4C, CH_3), 19.68 (4C, CH_2), 24.02 (4C, CH_2), 58.88 (4C, CH_2), 62.27 (1C, =CH_2, $^1J_{Pt-C}$ = 181 Hz), 63.32 (1C, CH_2), 89.62 (1C, =CH, $^1J_{Pt-C}$ = 189 Hz).

$Bu_4N[PtCl_3(CH_2CHSiMe_3)]$. ^{1}H NMR: 0.28 (s, 9H), 1.04 (t, 12H), 1.48 (m, 8H), 1.66 (m, 8H), 3.28 (m, 8H), 4.61 (m, 1H), 4.66 (m, 1H), 4.92 (m, 1H). ^{195}Pt NMR: −2663. ^{13}C NMR: 0.46 (2C, CH_3), 13.70 (4C, CH_3), 19.68 (4C, CH_2), 24.08 (4C, CH_2), 58.86 (4C, CH_2), 73.01 (1C, =CH_2, $^1J_{Pt-C}$ = 186 Hz), 80.69 (1C, = CH, $^1J_{Pt-C}$ = 195 Hz).

$Bu_4N[PtCl_3(C_8H_{14})]$. ^{1}H NMR: 1.02 (t, 12H), 1.40 (m, 8H), 1.48 (m, 8H), 1.68 (m, 8H), 2.16 (m, 2H), 2.43 (m, 2H), 3.28 (m, 8H), 5.05 (tm, 2H, $^{1.5}J_{Pt-H}$ = 67 Hz). ^{195}Pt NMR: −2681. ^{13}C NMR: 13.73 (4C, CH_3), 19.74 (4C, CH_2), 24.14 (4C, CH_2), 26.22 (2C, CH_2), 27.62 (2C, CH_2), 28.72 (2C, CH_2), 58.95 (4C, CH_2), 85.74 (2C, =CH, $^1J_{Pt-C}$ = 190 Hz).

NMR measurements

^{1}H and ^{195}Pt NMR spectra were recorded at 295 K in $CDCl_3$ on a Varian Unity 300 spectrometer working at 299.78 and 64.27 MHz respectively. The ^{1}H chemical shifts are reported in ppm, the spectra were calibrated on the residual $CHCl_3$ peak (δ = 7.25 ppm) as internal standard. The ^{195}Pt spectra were recorded with a WALTZ-16 proton decoupling sequence and the peak resonances are reported in ppm relative to K_2PtCl_6 (1 g H_2PtCl_6 in 3 ml 1 M HCl containing 50% D_2O, δ = 0 ppm) as external reference. ^{13}C spectra were recorded at 295 K in $CDCl_3$ on a 300 MHz Buker spectrometer operating at 75.47 MHz. The spectra were calibrated on the solvent peak at 77.0 ppm.

Low temperature unit

The Hi-Tech Ltd (Salisbury, UK) CryoFlow temperature option was attached to a Hi-Tech SF-61DX-2 diode-array stopped-flow system. This low temperature option comprises a well insulated, thermostated beaker which provides temperature control (±0.2 °C) of the sample flow lines and the observation cell. Within this vessel methanol as thermostating agent was used to maintain temperature control of the flow circuit components by circulating around the cell block and reagent line plumbing. The temperature of the thermostating agent was set and controlled by a proportional controller within the system operating a heat–cool strategy. Cooling was provided by a refrigeration coil immersed in the beaker unit and connected to a self contained vapour-compression refrigeration unit; heating was accomplished with an electrical immersion heater. A small plunger pump provides circulation of the thermostating agent between the cell block and the main body of the beaker. The delivery of reagents to the low temperature unit was achieved by making an umbilical connection to the standard Hi-Tech SF-61 DX-2 sample-handling unit where the cell block had been removed and replaced by a connection manifold. This way, the reagents were forced by the pneumatically driven syringes into the low temperature mixer/cell arrangement and the reacted solution was fed back to the stop syringe assembly. The dead time of the mixing unit is estimated to be less than 2 ms.

Kinetic measurements

Based on spectra of reactants and products, the following wavelengths were selected to monitor the reactions between **1** and the different nucleophiles: 300 (Br^-), 330 (I^-), 295 (N_3^-) and 320 nm (SCN^-). The total concentration of platinum was 0.50 mmol dm^{-3} and nucleophile concentrations were always at least ten times larger after mixing to ensure pseudo first-order reaction conditions. The ionic strength was kept constant at either 0.20 mol dm^{-3} (Br^- and I^-) or 0.05 mol dm^{-3} (Br^-, N_3^- and SCN^-). Temperature variations on **1** were performed between 223 and 243 K for Br^-, I^- and N_3^- while reaction with SCN^- only could be monitored at 223 K due to its extremely high reactivity. Fig. 1 shows typical kinetic runs at 223 K for

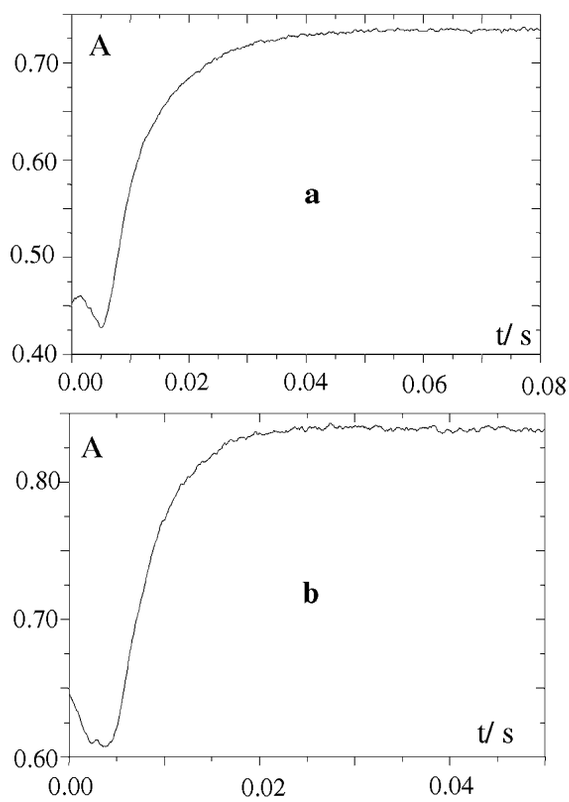

Fig. 1 Kinetic traces at 223 K and $[Y]^-$ = 10 mmol dm^{-3} for a) **1** + I^-, k_{obs} = 132(1) s^{-1}, b) **1** + N_3^-, k_{obs} = 243(2) s^{-1}.

reaction of **1** with I^- and N_3^-. Even if the half lives of some reactions observed were of the same order of magnitude as the dead time of the instrument, it was possible to derive rate constants since (1) the absorbance changes were sufficiently large to allow observation of the reactions for several half lives, and (2)

the half lives of first-order reactions are independent of concentration.

Reactions between complexes **2**, **3** and **4** and iodide were investigated at 330–335 nm and temperatures between 223 and 243, 223 and 253, and 223 and 263 K, respectively, once again the high reactivity limiting investigation at higher temperatures. The reactions were performed under pseudo first-order conditions using a total platinum concentration of 0.50 mmol dm^{-3} in all cases. The ionic strength was kept constant at 0.20 mol dm^{-3}.

The kinetic traces for all reactions investigated showed well-defined first-order behaviour with the substitution process *trans* to ethene being several orders of magnitude faster than substitution of the *cis* chlorides. Thus all reactions studied are described by eqn. (1), where L denotes the olefin:

$$[PtCl_3(L)]^- + Y \longrightarrow \textit{trans}\text{-}[PtCl_2Y(L)]^- + Cl^- \qquad (1)$$

Data were collected and observed pseudo first-order rate constants calculated using the Hi-Tech software package KinetAsyst2.[7] All least-squares fits were performed using SCIENTIST,[8] the observed pseudo first-order rate constants were fitted *versus* the ligand concentrations using a linear model, while activation parameters were calculated using the exponential form of the Eyring equation. Complete kinetics primary data are given as ESI. †

Equilibrium measurements

The MeOH solvento analogues of complexes **2**–**4** were prepared by abstraction of the chloride *trans* to the olefin as described previously.[4] UV–Vis spectra were recorded at 298.2 K on a Cary 300 Bio UV/Vis spectrophotometer after mixing of pre-thermostated solutions of the platinum solvento complexes and chloride solutions in 1.00 cm quartz cells in the thermostated cell compartment. Equilibrium constants were calculated by use of the SCIENTIST[8] non-linear least-squares minimising program. Complete absorbance/concentration data are given as ESI. †

Crystallography

Crystals of the tetrabutylammonium salt of **3**, suitable for X-ray diffraction, were obtained by addition of diethyl ether to a concentrated solution of the compound in dichloromethane. Slow evaporation yielded bright yellow plates. Crystals of the tetrabutylammonium salt of **4** were obtained by direct evaporation of the acetone reaction mixture used for preparation of the salt. The intensity data collections were done on a Siemens SMART CCD diffractometer using Mo K_α (0.71073 Å) and ω-scans at 293(2) K. All reflections were merged and integrated using SAINT[9] and were corrected for Lorentz, polarization and absorption effects with SADABS.[10] After completion of the data collections the first 50 frames were repeated to check for decay of which none was observed. The structures were solved by the heavy atom method and refined through full-matrix least squares cycles using the SHELXL97[11] software package with $\Sigma(|F_o| - |F_c|)^2$ being minimised. All non-H atoms were refined with anisotropic displacement parameters while the H atoms were constrained to parent sites using a riding model. The olefinic H atoms of $[Bu_4N]$[**3**] could not be detected from the Fourier map and were hence excluded from the final refinement while those of $[Bu_4N]$[**4**] were refined with individual isotropic thermal parameters. In both structures the minimum and maximum electron densities were located within 1 Å of the platinum atom. The graphics were done with the DIAMOND[12] Visual Crystal Structure Information System software.

CCDC reference numbers 176914 and 176915.

See http://www.rsc.org/suppdata/dt/b2/b200197g/ for crystallographic data in CIF or other electronic format.

Results and discussion

Kinetics and mechanism

Plots of observed rate constants *vs.* the concentration of excess nucleophiles are given in Fig. 2 and Eyring plots based on second-order rate constants in Fig. 3.

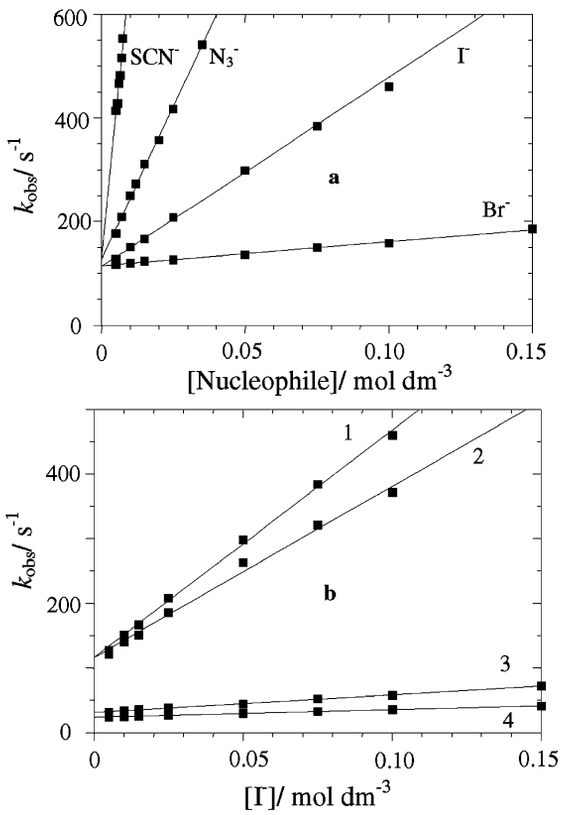

Fig. 2 (a) Concentration dependence of k_{obs} for reaction of **1** with Br^-, I^-, N_3^- and SCN^- at 223 K. (b) Iodide concentration dependence of k_{obs} for reaction with **1**, **2**, **3** and **4** at 223 K.

The intercepts of the plots in Fig. 2a are the same for the various nucleophiles within experimental error. Therefore, they correspond to the contribution from a common solvent path and not from reversible processes. Thus, all reactions proceed in accordance with the usual two-term rate law for square-planar substitution reactions as given by eqn. (2), where k_2 refers to the direct substitution process and k_1 to the solvent assisted pathway:

$$k_{obs} = k_1 + k_2[Y] \text{ with } k_1 = k_{MeOH}[MeOH] \qquad (2)$$

Even though complexes **1**–**4** are solvolysed to some extent already at the start of the kinetic runs, there was always a sufficient amount of $[PtCl_3(L)]^-$ present in solution to give a large enough absorbance change for all the reactions investigated. Since the solvento complexes are orders of magnitude more reactive than the parent chloro complexes (*cf.* data for k_{-1} in Table 3 below) their anation reactions are too fast to be observed even at 223 K. Thus, the observed absorbance changes are only due to the reactions of the parent chloride complexes with the various nucleophiles.

Second-order rate constants and activation parameters for reaction between complex **1** and the various nucleophiles at 223 K are summarised in Table 1. The order of reactivity based on the values of k_2 and k_{MeOH} in Table 1 is MeOH < Br^- < I^- < N_3^- < SCN^-, or in relative numbers about 1 : 100 : 700 : 2500 : 12000. This series corresponds to a normal nucleophilic discrimination for these ligands at this low temperature. Extrapolation of the rate constants for reaction between **1** and

Table 1 Rate constants at 223 K and activation parameters for the reactions between **1** and nucleophiles Y^-

Y^-	$10^{-3}k_2$/ $mol^{-1}\ dm^3\ s^{-1}$	$\Delta H_2^{\neq}$/ $kJ\ mol^{-1}$	$\Delta S_2^{\neq}$/ $J\ K^{-1}\ mol^{-1}$	k_1/s^{-1}	k_{MeOH}/ $mol^{-1}\ dm^3\ s^{-1}$	$\Delta H_{MeOH}^{\neq}$/ $kJ\ mol^{-1}$	$\Delta S_{MeOH}^{\neq}$/ $J\ K^{-1}\ mol^{-1}$
Br[a]	0.509(16)	21(2)	−96(9)	111(1)	4.5(1)	26(1)	−114(3)
Br[b]	0.520(18)			107(1)	4.3(1)		
I[a]	3.51(7)	17(1)	−98(4)	116(5)	4.7(2)	23(2)	−125(8)
N_3[b]	11.8(2)	11.9(1.5)	−111(6)	127(4)	5.1(2)	21(3)	−134(10)
SCN[b]	56(4)			129(23)	5.2(9)		

[a] $I = 0.200\ mol\ dm^{-3}$. [b] $I = 0.050\ mol\ dm^{-3}$.

Table 2 Rate constants at 223 K and activation parameters for the reactions between **1**, **2**, **3** and **4** and iodide

	$10^{-3}k_2$/ $mol^{-1}\ dm^3\ s^{-1}$	$\Delta H_2^{\neq}$/$kJ\ mol^{-1}$	$\Delta S_2^{\neq}$/ $J\ K^{-1}\ mol^{-1}$	k_1/s^{-1}	k_{MeOH}/ $mol^{-1}\ dm^3\ s^{-1}$	$\Delta H_{MeOH}^{\neq}$/ $kJ\ mol^{-1}$	$\Delta S_{MeOH}^{\neq}$/ $J\ K^{-1}\ mol^{-1}$
1	3.51(7)	17(1)	−98(4)	116(5)	4.7(2)	23(2)	−125(8)
2	2.65(6)	19.9(1.2)	−88(5)	116(5)	4.7(2)	24.4(1.3)	−120(5)
3	0.273(5)	24.6(1.7)	−84(7)	31.0(3)	1.256(1.2)	28.4(6)	−114(2)
4	0.119(2)	24(3)	−93(10)	23.6(1)	0.956(5)	29.9(8)	−108(3)

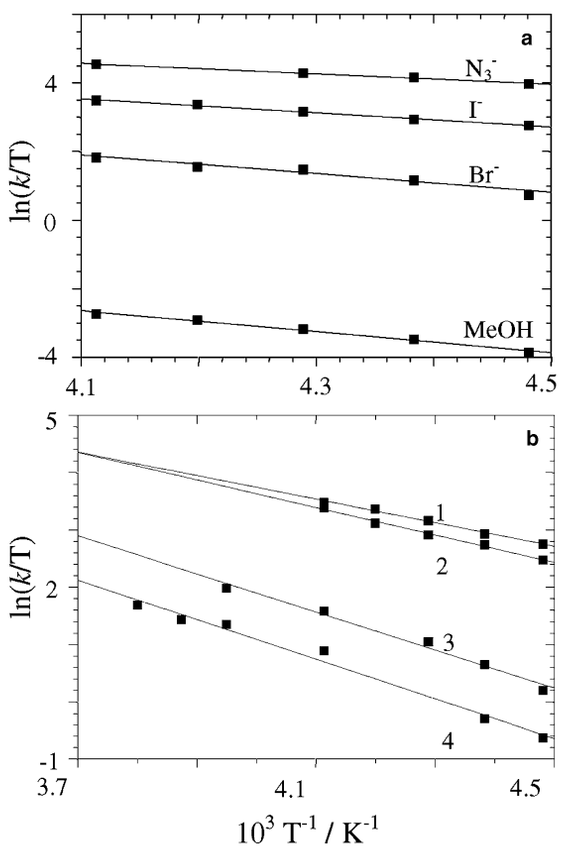

Fig. 3 Eyring plots for (a) the reactions of MeOH, Br^-, I^-, and N_3^- with **1**, (b) the reactions of I^- with **1**–**4**.

methanol, bromide, iodide and azide to 25 °C by use of the activation parameters in Table 1 and incorporation of the rate constant for reaction between **1** and ethene ($2100\ mol^{-1}\ dm^3\ s^{-1}$)[4] gives a much more compressed range of nucleophilicity $MeOH < C_2H_4 < Br^- < I^- < N_3^-$ of *ca.* 1 : 12 : 80 : 270 : 500 at ambient temperature. Thus, the nucleophilic discrimination of this particular complex is clearly temperature dependent. It is also noteworthy that ethene is low in the nucleophilicity series. A similar poor nucleophilicity of ethene has been noted earlier for reactions between platinum(II) complexes and ethene in aqueous solution.[13]

As observed previously for reactions of ethene complexes,[4] the activation entropies are largely negative. Between *ca.* 60 and 70% of the free energies of activation are due to the entropy contributions (*vide infra*).

Rate constants and activation parameters for reaction between complexes **1**–**4** and iodide are given in Table 2. Also here, the entropy terms are largely negative, amounting to between 50 and 60% of the overall free energy of activation. The order of reactivity for the four olefin complexes with I^- and MeOH based on the values of k_2 and k_{MeOH} in Table 2 is:

$$C_2H_4 \sim CH_2CHCH_2OH > CH_2CHSiMe_3 \sim C_8H_4 \quad (3)$$

spanning a factor of *ca.* 30 for iodide and *ca.* 5 for methanol as nucleophile. This trend reflects a slight variation in *trans* effect of these four olefinic ligands, which can be traced back to differences in bonding and stereochemistry (*vide infra*). Also in this case, however, extrapolation of the rate constants to 25 °C leads to a decrease in the span of nucleophilic discrimination (to factors of *ca.* 2 and 8 only for k_{MeOH} and k_2, respectively).

The equilibria between the various parent chloro complexes and their respective solvento analogues can be expressed by eqn. (3):

$$[PtCl_3(L)] + S \underset{k_{-1}}{\overset{k_1}{\rightleftharpoons}} [PtCl_2(L)S]^- + Cl^- \quad (3)$$

where k_1 and k_{-1} denote the rate constants for the forward and reverse reactions and the equilibrium constant K_{Cl} is defined by eqn. (4):

$$K_{Cl} = k_1/k_{-1} \quad (4)$$

Values of K_{Cl} for complexes **2**–**4** were calculated by least-squares fitting of eqns. (5) and (6) to the experimental concentration/absorbance data

$$K_{Cl} = [PtCl_2(L)(S)][Cl^-]/[PtCl_3(L)^-] \quad (5)$$

$$A_{obs} = C_{Pt}(\varepsilon_1 + \varepsilon_2 K_{Cl}^{-1}[Cl^-])(1 + K_{Cl}^{-1}[Cl^-]) \quad (6)$$

where ε_1 and ε_2 denote the molar absorptivities of the solvento and parent chloro complexes, respectively. The equilibrium concentrations of $[PtCl_3(L)]^-$, $[PtCl_2(L)(S)]$ and Cl^- were calculated for each concentration of added chloride using eqn. (7)

$$K_{Cl}^{-1}[Cl^-]^2 + (K_{Cl}^{-1}C_{Pt} - K_{Cl}^{-1}[Cl^-]_{add} + 1)[Cl^-] - [Cl^-]_{add} = 0 \quad (7)$$

where C_{Pt} and $[Cl^-]_{add}$ represent the total concentration of platinum (*i.e.* $C_{Pt} = [PtCl_3(L)]^- + [PtCl_2(L)(S)]$) and the concentration of added chloride, respectively.

Table 3 Comparison of forward[14] and reverse[15] second order rate constants as defined by eqns. (2) and (3)

L	k_{MeOH}/mol^{-1} dm^3 s^{-1}	$10^{-3}\,k_{-1}$/mol^{-1} dm^3 s^{-1}
SMe_2	$(6.1 \pm 1.2) \times 10^{-5}$ [a]	
SEt_2	$(8.5 \pm 0.8) \times 10^{-5}$ [b]	0.00126 [f]
Me_2SO	$(33.2 \pm 1.2) \times 10^{-5}$ [c]	0.0124 [f]
$AsEt_3$	0.026 ± 0.019 [d]	0.0522 [f]
PMe_3	0.21 ± 0.02 [d]	0.0836 [f]
PEt_3	0.27 ± 0.03 [d]	
PBu_3	0.21 ± 0.02 [d]	
PPh_3	0.13 ± 0.02 [d]	0.190 [f]
$P(OMe)_3$	0.42 ± 0.12 [d]	
C_2H_4	171 ± 19 [e]	6700 [g]
CH_2CHCH_2OH	185 ± 20 [e]	35100 [h]
$CH_2CHSiMe_3$	73 ± 8 [e]	12100 [i]
C_8H_{14}	76 ± 8 [e]	4200 [j]

[a] 30 °C; H^+ = 0.10 mol dm^{-3}; I = 0.50 mol dm^{-3}. [b] 30 °C; I = 0.50 mol dm^{-3}. [c] 30 °C; Cl^- = 0.025 mol dm^{-3}; I = 0.50 mol dm^{-3}. [d] 30 °C; LiCl = 0.48 mol dm^{-3}; I = 0.48 mol dm^{-3}. [e] MeOH; Extrapolated to 25 °C; I = 0.20 mol dm^{-3}. [f] In 95% MeOH + 5% H_2O at 25 °C, no constant ionic strength. [g] Estimated from $K_{Cl} = (6.3 \pm 0.8) \times 10^{-4}$ mol^{-1} dm^3 (from ref. 4) and $k_1 \sim 4000$ s^{-1}. [h] Estimated from $K_{Cl} = (1.30 \pm 0.13) \times 10^{-4}$ mol^{-1} dm^3 and $k_1 \sim 4600$ s^{-1}. [i] Estimated from $K_{Cl} = (1.49 \pm 0.13) \times 10^{-4}$ mol^{-1} dm^3 and $k_1 \sim 1800$ s^{-1}. [j] Estimated from $K_{Cl} = (4.5 \pm 0.4) \times 10^{-4}$ mol^{-1} dm^3 and $k_1 \sim 1900$ s^{-1}.

Table 4 Crystal data and structure refinement for the tetrabutylammonium salts of **3** and **4**

	Bu_4N[**3**]	Bu_4N[**4**]
Empirical formula	$C_{21}H_{48}Cl_3SiNPt$	$C_{24}H_{50}Cl_3NPt$
Formula weight	644.13	654.09
Crystal system	Triclinic	Monoclinic
Space group	$P\bar{1}$	$P2_1/n$
a/Å	9.0976(18)	14.731(3)
b/Å	13.448(3)	9.4487(19)
c/Å	13.449(3)	21.021(4)
α/°	99.16(3)	90
β/°	104.48(3)	91.94(3)
γ/°	109.64(3)	90
V/Å^3	1446.2(5)	2924.2(10)
Z	2	4
D_c/g cm^{-3}	1.479	1.486
μ/mm^{-1}	5.177	5.083
T_{max}/T_{min}	0.422/0.150	0.785/0.236
$F(000)$	648	1320
θ limit/°	2.41 to 27.48	1.66 to 31.83
Index ranges	$-11 \le h \le 11$	$-21 \le h \le 20$
	$-17 \le k \le 17$	$-8 \le k \le 13$
	$-17 \le l \le 17$	$-29 \le l \le 29$
Reflections collected/unique	10481/6628	29582/9167
R_{int}	0.0479	0.0802
Observed reflections ($I > 2\sigma(I)$)	4874	6441
Data/restraints/parameters	6628/0/256	9167/0/276
S	0.977	0.998
($I > 2\sigma(I)$) R	0.0562	0.0431
wR	0.1350	0.1080
(all data) R	0.0784	0.0684
wR	0.1410	0.1202
$\Delta\rho_{max}$; $\Delta\rho_{min}$/e Å^{-3}	2.701; −2.304	2.323; −1.883

Values of rate constants k_{MeOH} and k_{-1} (calculated by use of the derived K_{Cl} values and eqn. (4)) as defined by eqn. (3) for complexes **1**–**4** are given in Table 3 together with data for some related systems. From these values, the following quantitative *trans*-effect series can be derived:

$$SR_2 < Me_2SO < AsEt_3 < PR_3 < P(OR)_3 < C_2H_4$$
$$1 : 5 : 400 : 3500 : 7000 : 3 \times 10^6$$

The *trans* effect series previously reported[2] for reactions of related platinum(II) complexes in aqueous solution is H_2O (1) < NH_3 (200) < Cl^- (330) < Br^- (3000) < DM*S*O (2×10^6) < C_2H_4 (~10^{11}). The present results (Table 3) show that the reactivity of **1** is indeed 5–6 orders of magnitude larger than that of the analogous sulfur-bonded DMSO complex.

Table 5 Selected bond lengths (Å) and angles (°) for the anions in **3** and **4** in their tetrabutylammonium salts

	3	**4**
Pt–Cl(1)	2.314(2)	2.3238(16)
Pt–Cl(2)	2.285(2)	2.3003(12)
Pt–Cl(3)	2.294(2)	2.3115(13)
Pt–C(1)	2.105(9)	2.147(4)
Pt–C(2)	2.161(9)	2.139(4)
C(1)–C(2)	1.437(13)	1.391(7)
Cl(1)–Pt–Cl(2)	89.24(10)	87.61(5)
Cl(1)–Pt–Cl(3)	89.43(10)	89.76(5)
Cl(2)–Pt–Cl(3)	178.49(9)	177.36(5)
Pt–C(2)–Si	121.4(5)	
Pt–C(1)–C(8)		118.5(3)
Pt–C(2)–C(3)		119.6(4)
Cl(1)–Pt–C(1)	155.9(3)	161.16(13)
Cl(1)–Pt–C(2)	164.6(3)	160.67(14)
Cl(2)–Pt–C(1)	92.0(3)	94.75(13)
Cl(2)–Pt–C(2)	93.2(3)	94.42(14)
Cl(3)–Pt–C(1)	88.9(3)	87.81(13)
Cl(3)–Pt–C(2)	88.2(3)	88.00(14)

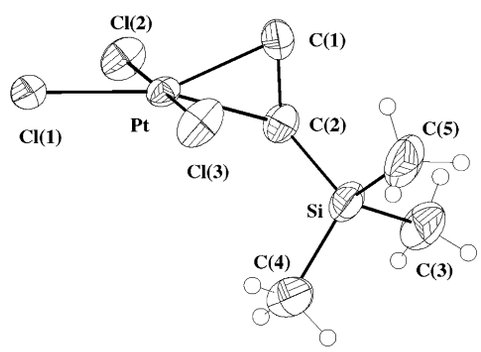

Fig. 4 Molecular structure showing the numbering scheme and thermal ellipsoids (30% probability level) for **3**, the hydrogen atoms are of arbitrary size.

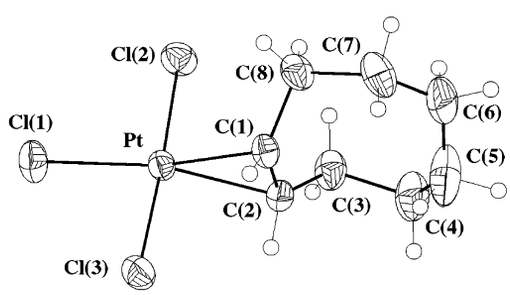

Fig. 5 Molecular structure showing the numbering scheme and thermal ellipsoids (30% probability level) for **4**, the hydrogen atoms are of arbitrary size.

Ground state structures

Crystal data, details of the data collection and refinement parameters for the tetrabutylammonium salts of **3** and **4** are summarised in Table 4. Molecular diagrams showing the numbering scheme and thermal ellipsoids of the complex anions **3** and **4** are given in Figs. 4 and 5. Selected bond distances and angles are summarised in Table 5.

The crystal structures of Bu_4N[**3**] and Bu_4N[**4**] are composed of discrete cation–anion pairs of Bu_4N^+ and $[PtCl_3(L)]^-$. The closest contacts in both structures are >3.6 Å indicating that the packing is governed by van der Waals forces alone and not by electronic interactions.

Table 6 Comparison of geometrical parameters for complexes of the type $[PtCl_3(L)]^-$

Complex	Pt–Cl/Å	Pt–C_1 [Pt–C_2]/Å	C_1–C_2/Å	Ref.
$K_2[PtCl_4]$	2.317(2)			17
$Et_4N[PtCl_3(MeCN)]$	2.266(2)			18
$Et_4N[PtCl_3(py)]$	2.305(2)			19
$Bu_4N[PtCl_3(CO)]$	2.289(3)			20
$K[PtCl_3(Me_2SO)]$	2.318(5)			21
$K[PtCl_3(NH_3)]$	2.321(7)			22
$K[PtCl_3(C_2H_4)]$	2.340(2)	2.128(3) [2.135(3)]	1.375(4)	23
$Bu_4N[PtCl_3(CH_2CHSiMe_3)]$	2.314(2)	2.105(9) [2.161(9)]	1.437(13)	This work
$Bu_4N[PtCl_3(C_8H_{14})]$	2.3238(16)	2.147(4) [2.139(9)]	1.391(7)	This work
$Ph_4P[PtCl_3(C_8H_{14})]$	2.3632(12)	2.160(4) [2.161(4)]	1.399(6)	24
$Et_4N[PtCl_3(CH_2CHOCH_2CH_3)]$	2.324(2)	2.128(7) [2.208(7)]	1.382(12)	25
$[PtCl_2(COD)]$[a]	2.312(1)	2.170(6)	1.381(8)	26
$[PtCl_2(CH_2CHC_6H_5)_2]$	2.310(2)	2.156(7) [2.270(5)]	1.382(9)	27
	2.304(2)	2.173(6) [2.258(6)]	1.398(9)	
$Et_4N[PtCl_3(PEt_3)]$	2.382(4)			28

[a] COD = *cis,cis*-1,5-cyclooctadiene.

The co-ordination complexes exhibit the expected square-planar geometry with the olefins co-ordinated perpendicular to the co-ordination plane as described by the Dewar–Chatt–Duncanson model.[16] The Pt–C(2)–Si angle of 121.4(5)° in **3** and the Pt–C(1)–C(8) and Pt–C(2)–C(3) angles of 118.5(3) and 119.6(4)° in **4** indicate a 'side-on' co-ordination mode of the olefins to the metal centre.

The cyclooctene molecule in **4** adopts a twisted chair conformation and points in the direction of Cl(3) resulting in a slight elongation of the Pt–Cl(3) bond distance as compared to Pt–Cl(2). In **3** the Pt–C(2) bond is significantly longer and the Pt–C(1) bond correspondingly shorter than in the simple symmetric ethene complex **1**. This asymmetry may be attributed to the bulky $SiMe_3$ substituent co-ordinated to C(2), and to the electron donor properties of this substituent. It is noteworthy that the two other complexes listed in Table 6 containing unsymmetrical olefin ligands ($CH_2CHOCH_2CH_3$ and CH_2-CHC_6H_5) also display distinctly different Pt–C bond distances, similar to that observed for **3**. In complexes **4** and **1**, on the other hand, with symmetric olefins, the Pt–C(1) and Pt–C(2) bond distances are the same within experimental errors. Furthermore, a slight elongation of the C(1)–C(2) bond distance in **3** as compared to that in **4** and related structures in Table 6 may also be due to the electron donor properties of the trimethylsilyl substituent at C(2) and eventully also to a larger extent of π-back bonding into the olefin antibonding orbitals in **3** than in **4**.

A very small, but significant, elongation of the Pt–Cl bond distances *trans* to the olefin ligands, compared to those in the *cis* positions, is observed. However, the amount of ground state bond weakening of the chloro ligands *trans* to the olefins is very small compared to that observed for most other *trans*-directing ligands listed in Table 6. Thus, the ground-state *trans* influence of these olefins is very small, due to the interplay between σ donation and π back donation. This is in agreement with the previously established *trans* influence sequence.[29]

The ^{13}C NMR spectra reveal some information on the structures of the complexes in solution, especially when interpreted with the solid state structures in mind. The spectra of complexes **1** and **4**, containing symmetrical olefin ligands, display single resonances for the chemically equivalent olefinic C atoms with single first order Pt–C coupling constants. In complexes **2** and **3** with chemically non-equivalent C atoms two sets of resonances are observed, corresponding to each of the C atoms, each displaying a unique first order Pt–C coupling constant. The resonances can be assigned to the respective C atoms based on their chemical shifts. For **1** the single resonance is observed at 68.22 ppm ($^1J_{Pt-C}$ = 193 Hz) and for **4** at 85.74 ppm ($^1J_{Pt-C}$ = 190 Hz). Each of the complexes **2** and **3** display one chemical shift close to 68 ppm, at 62.27 ($^1J_{Pt-C}$ = 181 Hz) and 73.01 ($^1J_{Pt-C}$ = 186 Hz) ppm, respectively, assigned to the $=CH_2$ moiety. The other chemical shift lies close to 86 ppm: at 89.62 ($^1J_{Pt-C}$ = 189 Hz) for **2** and at 80.69 ($^1J_{Pt-C}$ = 195 Hz) ppm for **3**, assigned to $=CH–CH_2OH$ and $=CH–SiMe_3$, respectively. In the crystal structures with unsymmetrical olefin ligands the bond distances between Pt and the substituted C atoms are significantly longer than those to the unfunctionalised ones (Table 6). This observation might be rationalised in terms of less effective back bonding from the metal centre to the antibonding orbital localised at the functionalised C atom. From these results it might seem peculiar that the longer Pt–C bond distances are associated with the larger Pt–C first order coupling constants. However, the first order coupling constants, as described by the Fermi contact term,[30] result predominantly from an overlap of the s orbitals of the respective nuclei. The same argument used to account for the longer Pt–C bond distances, *i.e.* an increased electron density on the functionalised C atom, is also applicable here. The more electron rich s orbital of the functionalised C atom would result in more effective s-orbital overlap with the platinum centre and hence result in the larger coupling constants observed.

Ground state *vs.* transition state effects

The structural data summarised in Tables 5 and 6 confirm that **3** and **4** are indeed very good model systems for **1**. The Pt–Cl bond distances *trans* to the olefins are essentially the same in the ground state within the error limits imposed on the structures by differences in counter ions and packing.[31] The crystal structures of Bu_4N[**3**], Bu_4N[**4**] and Ph_4P[**4**][23] show Pt–Cl bond distances of 2.314(2), 2.3238(16) and 2.3632(12) Å, respectively—similar to those found *trans* to ethene in $[PtCl_3(C_2H_4)]^-$ and in other olefinic complexes reported in the literature. Note that the Pt–Cl distances in the olefin complexes are not very different from those *trans* to chloride in $[PtCl_4]^{2-}$, indicating similar bond strengths in the ground state. In spite of this, the difference in rate of substitution of chloride ligands between $[PtCl_4]^{2-}$ and $[PtCl_3(C_2H_4)]^-$ is at least nine orders of magnitude.[32] Since the ground state bond strengths are similar, this extreme difference in rate can only be rationalised in terms of transition state stabilisation in the case of the olefin complexes. Such stabilisation is accompanied by large negative activation entropies, as found for the fast substitution processes studied here. The $-T\Delta S^{\neq}$ contributions to the overall free energy of activation for the reactions studied amount to between 50 and 70%, compared to only a few percent for substitution processes *trans* to chloride, for instance.

A closer comparison of the rate and structural data for the four olefin complexes investigated shows some minor but still significant differences. Complexes **1** and **2** react between 5 and

30 times faster than **3** and **4**. A small, but steady, increase of the free energies of activation is observed for the reactions of **1**–**4** with iodide as incoming nucleophile with values of 46 ± 1.3, 46.2 ± 1.6, 50 ± 2 and 52 ± 3 kJ mol^{-1}, respectively. The *trans* effect sequence ethene > allyl alcohol > vinyltrimethylsilane > cyclooctene parallels an increase in the bulkiness of the olefins and an increase in the electron donor capacity of the olefin substituents, affecting back bond stabilisation, in particular in the transition state. This decrease in reactivity cannot be traced back to differences in ground state labilisation of the *trans* chloride ligands (*cf.* Table 6).

Conclusion

Low-temperature stopped-flow spectroscopy has allowed studies of extremely fast substitution processes in methanol *trans* to olefins in some classical non-hindered square-planar systems. These fast processes follow the usual two-term rate law typical for square-planar complexes at ambient conditions, and the mode of activation is associative, as indicated by their sensitivity to the nature of the entering ligand and their negative entropies of activation. The very fast reactions *trans* to the olefins are due to transition state stabilisation, whereas ground state destabilisation as displayed by crystallographic bond length changes is of minor importance. The processes are characterised by an unusually large contribution of the entropy term to the overall free energy of activation. The experimental data have for the first time allowed a quantitative evaluation of the *trans* effect of the olefins, which is *ca*. 10^{11} times that of water and *ca.* 10^{6} times that of sulfur-bonded dimethylsulfoxide.

Acknowledgements

Thanks are due to Mr. E.J. King, Hi-Tech Ltd., Salisbury, UK for valuable technical assistance in connection with installation of the cryo unit. Mr. Fredric Pilz is acknowledged for the preparation of Bu_4N[**4**]. Financial support from the Swedish Science Council (VR) and the Swedish International Development Cooperation Agency (SIDA), including a post-doctoral fellowship at Lund for S. O. is gratefully acknowledged. The Crafoord Foundation is thanked for funding of the cryo stopped-flow and diode array units.

References

1 F. R. Hartley, *Comprehensive Organometallic Chemistry*, Pergamon Press, 1982, vol. 6, p. 471.
2 L. I. Elding and Ö. Gröning, *Inorg. Chem.*, 1978, **17**, 1872.
3 L. Canovese, M. L. Tobe and L. Cattalini, *J. Chem. Soc., Dalton Trans.*, 1985, 27.
4 M. R. Plutino, S. Otto, A. Roodt and L. I. Elding, *Inorg. Chem.*, 1999, **38**, 1233.
5 P. B. Chock, J. Halpern and F. E. Paulik, *Inorg. Synth.*, 1973, **14**, 90.
6 E. M. Haschke and J. W. Fitch, *J. Organomet. Chem.*, 1973, **57**, C93.
7 KinetAsyst2; Version 2.2, Hi-Tech Limited, Salisbury, UK, 1999.
8 SCIENTIST, Program for Least-Squares Parameter Optimization, MicroMath Scientific Software, Utah, 1990.
9 SAINT, Siemens Analytical X-ray Instruments Inc., Madison, Wisconsin, USA, 1995.
10 G. M. Sheldrick, SADABS, University of Göttingen, Germany, 1996.
11 G. M. Sheldrick, SHELXL97, University of Göttingen, Germany, 1997.
12 K. Brandenburg, DIAMOND, Version 2.1, Crystal Impact, Bonn, Germany, 1997.
13 L. I. Elding and A.-B. Gröning, *Inorg. Chim. Acta*, 1980, **38**, 59.
14 R. Gosling and M. L. Tobe, *Inorg. Chem.*, 1983, **22**, 1235.
15 M. L. Tobe and A. T. Treadgold, *J. Chem. Soc., Dalton Trans.*, 1988, 2347.
16 J. Chatt and L. A. Duncanson, *J. Chem. Soc.*, 1953, 2939 and references therein.
17 R. H. B. Mais, P. G. Owston and A. M. Wood, *Acta Crystallogr., Sect. B*, 1972, **28**, 393.
18 V. Y. Kukushkin, I. A. Krol, Z. A. Starikova and V. M. Tkachuk, *Koord. Khim.*, 1990, **16**, 1406.
19 V. K. Belsky, V. Y. Kukushkin, V. E. Konovalov, A. I. Moiseev and V. N. Yakovlev, *Zh. Obsch. Khim.*, 1990, **60**, 2180.
20 D. R. Russel, P. A. Tucker and S. Wilson, *J. Organomet. Chem.*, 1976, **104**, 387.
21 R. Melanson, J. Hubert and F. D. Rochon, *Acta Crystallogr., Sect. B*, 1976, **32**, 1914.
22 V. Y. Kukushkin, V. K. Belsky, V. E. Konovalov, E. A. Aleksandrova, E. Yu. Pankova and A. I. Moiseev, *Phosphorus Sulfur Silicon*, 1992, **69**, 103.
23 R. A. Love, T. F. Koetzle, G. J. B. Williams, L. C. Andrews and R. Bau, *Inorg. Chem.*, 1975, **14**, 2653–2657.
24 S. Otto, A. Roodt and L. I. Elding, manuscript in preparation.
25 R. C. Elder and F. Pesa, *Acta Crystallogr., Sect. B*, 1978, **34**, 268.
26 A. Syed, E. D. Stevens and S. G. Cruz, *Inorg. Chem.*, 1984, **23**, 3673.
27 A. Albinati, W. R. Caseri and P. S. Pregosin, *Organometallics*, 1987, **6**, 788–793.
28 G. W. Bushnell, A. Pidcock and M. A. R. Smith, *J. Chem. Soc., Dalton Trans.*, 1975, 572.
29 S. Otto and M. H. Johansson, *Inorg. Chim. Acta*, 2002, **329**, 135.
30 T. G. Appleton and M. A. Bennet, *Inorg. Chem.*, 1978, **17**, 738.
31 Z. Bugarcic, K. Lövqvist and Å. Oskarsson, *Acta Chem. Scand.*, 1993, **47**, 554.
32 L. I. Elding, *Acta Chem. Scand.*, 1966, **20**, 2559.